INSTITUTE OF PHYSICS PUBLISHING JOURNAL OF PHYSICS: CONDENSED MATTER

J. Phys.: Condens. Matter **14** (2002) 9153–9169 PII: S0953-8984(02)36567-6

Phase transitions and critical behaviour of simple fluids and their mixtures

Gerhard Kahl[1], **Elisabeth Schöll-Paschinger**[1] **and George Stell**[2]

[1] Institut für Theoretische Physik and CMS, TU Wien,, Wiedner Hauptstraße 8–10, A-1040 Wien, Austria
[2] Department of Chemistry, State University of New York, Stony Brook, NY 11794-3400, USA

Received 2 May 2002
Published 27 September 2002
Online at stacks.iop.org/JPhysCM/14/9153

Abstract

It has become clear that the self-consistent Ornstein–Zernike approximation (SCOZA) is a microscopic liquid-state theory that is able to predict the location of the critical point and of the liquid–vapour coexistence line of a simple fluid with high accuracy. However, applications of the SCOZA to continuum systems have been restricted up to now to liquids where the interatomic potentials consist of a hard-core part with an attractive two-Yukawa-tail part. We present here a reformulation of the SCOZA that is based on the Wertheim–Baxter formalism for solving the mean-spherical approximation for a hard-core–multi-Yukawa-tail fluid. This SCOZA version offers more flexibility and opens access to systems where the interactions can be represented by a suitable linear combination of Yukawa tails. We demonstrate the power of this generalized SCOZA for a model system of fullerenes; furthermore, we study the critical behaviour of a system with an explicitly density-dependent interaction where the phenomenon of double criticality is observed. Finally, we extend our SCOZA version to the case of a binary symmetric mixture and present and discuss results for phase diagrams.

1. Introduction

During the past few decades liquid-state physicists have devoted much effort to the development of microscopic theories that allow the calculation of the structural and thermodynamic properties of simple liquids (and their mixtures) with high accuracy (for an overview see, for instance, [1, 2]). The development of such concepts at a high level of sophistication in combination with very accurate numerical algorithms has brought us to a position where for large parts of the density–temperature plane these methods produce results that are practically indistinguishable from data obtained in computer simulations. However, this success is no longer guaranteed as we leave the liquid-state region and approach the liquid–gas coexistence curve and/or the critical region where typically the following problems are observed: the shape

 © 2002 IOP Publishing Ltd Printed in the UK

of the coexistence curve is not reproduced correctly—sometimes its two branches are even left unconnected in the critical region; critical points are not located correctly; and the related critical exponents do not agree with the exact ones.

The fact that an exact localization of the phase boundaries and an accurate determination of the critical properties is not within reach for conventional microscopic liquid-state theories is of course highly unsatisfactory. Therefore, again much effort has been dedicated during the past few years to the development of advanced microscopic liquid-state theories that remain successful even in the critical region: at present, two concepts are available that were specially developed to cope with the problems encountered in the critical region and near the phase boundaries. One is the self-consistent Ornstein–Zernike approximation (SCOZA), proposed by Stell and Høye in the 1970s [3, 4], and reformulated in different versions in subsequent work with several co-authors (for a recent presentation see, for instance, [5, 6]). The other concept is the hierarchical reference theory (HRT), due to Reatto and co-workers [7]. Both theories try to cope with the difficulties encountered in the critical region with different strategies: while the HRT merges concepts of renormalization group theory with theoretical liquid-state approaches, the SCOZA starts from a generalized mean-spherical ansatz, enforcing consistency between different thermodynamic routes. The high level of sophistication of these two concepts (compared to conventional techniques) leads of course to considerably more complex formalisms which, in turn, cause substantial numerical and computational problems.

In this contribution we shall focus on the SCOZA and present a generalization of its formalism which allows a broader applicability for continuum systems. Although the SCOZA was proposed more than 20 years ago, practical applications are, as a consequence of the complexity of its formalism, still rather scarce. Its real breakthrough came in 1996 [8], when a reformulation of the SCOZA partial differential equation (PDE) made access to subcritical temperatures possible. Since then, the SCOZA has been applied to a few discrete [8–15] and continuum systems [5, 6, 16]. Here we focus on the continuum case, where applications have been restricted up to now to the one-component case and to hard-core (HC) interactions with an adjacent attractive potential built up by linear combination of up to two Yukawa tails (offering the possibility to approximate a Lennard-Jones (LJ) interaction rather accurately [6]). The binary case has been heretofore treated only in the special context of decorated lattice models that are isomorphic to the nearest-neighbour Ising model [15].

From present SCOZA applications we know the following: the liquid–vapour branches and the critical point are localized very accurately (within 1–2% of the best numerical estimates). Various effective critical exponents (defined as slopes of curves of logarithmic plots) were investigated and it was found that they are very close to the estimated exact form except very close to the critical point. Above the critical point the theory yields the same critical exponents as the spherical model but this regime is very narrow, so the thermodynamics and effective exponents are in good agreement with the true critical behaviour until the temperature differs from its critical value by $\leqslant 1\%$. On the coexistence curve, on the other hand, the exponents are neither spherical nor classical and turn out to be very accurate. An analytic study of the SCOZA critical exponents and the scaling behaviour in three dimensions was given by Høye *et al* [17]: it was seen that standard scaling is not fulfilled, but rather a generalized form of scaling.

The limitation of the SCOZA to HC–two-Yukawa-tail interactions can be traced back to the availability of the semi-analytic solution of the mean-spherical approximation (MSA) for such a system [4, 18]: the analytic expressions represent a very valuable framework and hence lead to considerable simplifications in the formalism and the implementation of the SCOZA. In contrast, SCOZA applications for an *arbitrary* potential which cannot benefit from the availability of an analytic framework and hence require a fully numerical treatment are—at

least for the moment—out of reach. In this contribution we propose a generalization of the SCOZA, that allows a broader application of this advanced liquid-state method. It is based on, instead of the Laplace-transform route used in [5], the more elegant and more flexible Wertheim–Baxter factorization route for solving the MSA for HC systems with a formally arbitrary number of Yukawa tails; the required expressions are summarized in [19]. Now a larger variety of realistic potentials come within reach, while fully maintaining the attractive features of the availability of the semi-analytic MSA solution: as long as these interactions are continuous, they can be approximated by a suitable linear combination of Yukawa tails. Further, we have extended the SCOZA to the binary case; practical applications are restricted, however (due to the high numerical costs), to the simplified symmetric binary mixture; again we benefit from the availability of the MSA solution for a mixture of HC–Yukawa-tail systems [19].

We first demonstrate the power of our generalization for the one-component case. Since previous studies have shown that the phase diagram of a LJ system can be predicted very accurately, we focus instead on another test system, i.e. on the model fullerenes C_{60} and C_{70}, described by the sphericalized Girifalco potential [20]. The interaction of this potential has a much stiffer repulsive part compared to the LJ interaction; its attractive well is much shorter ranged and much deeper. These features lead to a very specific phase diagram (the question of the existence of a liquid state is not yet completely settled) and to numerical problems in other advanced liquid-state methods [21]. In contrast, the SCOZA, however, is able to reproduce the localization of the critical point as predicted in computer experiments with high accuracy.

We then study the phase behaviour of a HC system with an explicitly density-dependent attractive Yukawa tail (introduced via a density-dependent inverse screening length) and obtain, for a particular form of the density dependence, phase diagrams with two first-order phase transitions (liquid–vapour and liquid–liquid), each with its own critical point. Finally we investigate the phase diagram of a binary symmetric mixture; we observe three archetypes of phase diagrams, characterized by the loci where the line of the second-order demixing transition (λ-line) intersects the first-order liquid–gas transition line. The sequence of these three types of phase diagram is triggered by a parameter α which is the ratio between the unlike and the like interactions.

This contribution is organized as follows. In the next section we introduce the main ideas of the generalized formalism of the SCOZA. In section 3 we apply this advanced liquid-state method to the systems mentioned above (both one- and two-component cases) and discuss the results. The paper is closed with concluding remarks.

2. Theory

In this contribution we shall restrict ourselves to systems with pair interactions $\Phi(r)$ consisting of a repulsive HC (diameter σ) and an adjacent attractive tail $w(r)$:

$$\Phi(r) = \begin{cases} \infty & r \leqslant \sigma \\ w(r) & r > \sigma. \end{cases} \tag{1}$$

In particular we focus on pair interactions that are linear combinations of Yukawa tails (labelled by Greek indices), i.e.

$$w(r) = \sum_{\nu} \frac{K_\nu}{r} \exp[-z_\nu(r-\sigma)]. \tag{2}$$

Further, we allow $w(r)$ to be explicitly density dependent ($w(r) = w(r;\rho)$), ρ being the number density. To be more specific, we introduce a density-dependent inverse screening length. In the binary case above, expressions generalize in a straightforward way: we now

have a set of three interactions $\Phi_{ij}(r)$, or $w_{ij}(r)$, characterized by a set of (additive) diameters σ_{ij} and contact values $K_{v;ij}$ $(i, j = 1, 2)$; we restrict ourselves to potentials with one Yukawa tail only. Further, the mixture is characterized by the total density ρ and the concentration x of species 1; partial number densities are defined via $\rho_1 = x\rho$ and $\rho_2 = (1 - x)\rho$.

2.1. SCOZA—the one-component case

The SCOZA is based on the OZ relation [22]

$$h(r) = c(r) + \rho \int \mathrm{d}\boldsymbol{r}'\, c(r')h(|\boldsymbol{r} - \boldsymbol{r}'|) \tag{3}$$

supplemented by a MSA-type closure relation, i.e. [8]

$$g(r) = 0 \qquad \text{for } r \leqslant \sigma \tag{4}$$

$$c(r) = c_{\mathrm{HC}}(r) + K(\rho, T)w(r) \qquad \text{for } r > \sigma. \tag{5}$$

$h(r)$ and $c(r)$ are the total and the direct correlation functions, $g(r) = h(r) + 1$ is the pair distribution function, and T is the temperature. $c_{\mathrm{HC}}(r)$ is the direct correlation function for the HC reference system for which we have chosen for convenience the Waisman parametrization [23], which is known to reproduce simulation results for the structural properties with high accuracy. For $r > \sigma$, $c_{\mathrm{HC}}(r) = K_0/r \exp[-z_0(r - \sigma)]$, where K_0 and z_0 are known functions of ρ (see appendix A of [5]). The state-dependent function $K(\rho, T)$ in (5) is not fixed *a priori* and is determined by the requirement of thermodynamic consistency between the energy and the compressibility route: let $\chi_{\mathrm{red}} = \rho k_{\mathrm{B}} T \chi_{\mathrm{T}}$ be the reduced (dimensionless) isothermal compressibility, given via the compressibility route by

$$(\chi_{\mathrm{red}})^{-1} = 1 - \rho\tilde{c}(q = 0) \tag{6}$$

where the tilde represents the Fourier transform; further, let u be the excess (over that of the ideal gas) internal energy per volume, given via the energy route by

$$u = 2\pi\rho^2 \int_\sigma^\infty \mathrm{d}r\, r^2 w(r)g(r); \tag{7}$$

if χ_{red} and u come from a unique Helmholtz free energy, then they are related via

$$\rho \frac{\partial^2 u}{\partial \rho^2} = \frac{\partial}{\partial \beta}\left(\frac{1}{\chi_{\mathrm{red}}}\right). \tag{8}$$

For the special choice of the pair interaction $w(r)$ (cf (2)) and if one uses the Waisman parametrization for $c_{\mathrm{HC}}(r)$, the SCOZA benefits from the availability of the semi-analytic solution of the MSA. Two different approaches to this solution have been proposed in the literature: the (original) Laplace-transform route [4, 18] and the Wiener–Hopf factorization technique introduced by Wertheim and Baxter [24, 25]. The first one uses a rather heavy formalism which leads to tractable expressions for up to two Yukawa tails; the latter approach is more elegant and more flexible and provides—even for an arbitrary number of Yukawa tails—compact expressions; they are summarized in [19] in a form suitable for numerical evaluation. Although there has been a great deal of important development of the application of the Baxter approach to the case of an arbitrary number of Yukawa tails (see [26–29] and references therein), we know of no formulation in the context of SCOZA or quantitative studies that are directly relevant to use in the SCOZA. In the following we outline the formulation of the SCOZA for many Yukawa potential tails using the Baxter approach, and refer the reader interested in a more detailed presentation to [30].

Under certain conditions [31], the solution of the OZ equation is equivalent to the solution of the following two integral equations:

$$2\pi r c(r) = -Q'(r) + \rho \int Q(t)\,Q'(r+t)\,\mathrm{d}t \tag{9}$$

$$2\pi r h(r) = -Q'(r) + 2\pi\rho \int (r-t)h(|r-t|)\,Q(t)\,\mathrm{d}t \tag{10}$$

introducing the so-called factor function $Q(r)$. For a system with n Yukawa tails the factor function is characterized by $(2n+2)$ as yet undetermined coefficients (a, b, C_ν, and D_ν), i.e.

$$Q(r) = Q^0(r) + \sum_\nu \frac{1}{z_\nu} D_\nu \mathrm{e}^{-z_\nu(r-\sigma)} \tag{11}$$

$$Q^0(r) = \begin{cases} \dfrac{a}{2}(r-\sigma)^2 + b(r-\sigma) + \displaystyle\sum_\nu \frac{1}{z_\nu} C_\nu[\mathrm{e}^{-z_\nu(r-\sigma)} - 1] & 0 < r < \sigma \\ 0 & r > \sigma. \end{cases} \tag{12}$$

Introducing further the G_ν via

$$G_\nu = z_\nu \int_\sigma^\infty r \exp[-z_\nu(r-\sigma)] g(r)\,\mathrm{d}r \tag{13}$$

one can derive (along with the MSA closure relation) a set of $2n$ non-linear equations for the $2n$ unknowns G_ν and D_ν: n of these equations are linear in the D_ν; their solution yields $D_\nu = D_\nu(\rho, G_\nu)$. Finally one can also relate a to these unknowns, leading thus to an expression $a = a(G_\nu, D_\nu)$; the relations are summarized in [19].

The factorization formalism leads to

$$(\chi_{\mathrm{red}})^{-1} = \left(\frac{a}{2\pi}\right)^2 \tag{14}$$

so (8) now becomes

$$\rho \frac{\partial^2 u}{\partial \rho^2} = 2\frac{a}{(2\pi)^2}\frac{\partial a}{\partial u}\frac{\partial u}{\partial \beta}. \tag{15}$$

Inserting $a = a(G_\nu, D_\nu)$ with $D_\nu = D_\nu(\rho, G_\nu)$ into the PDE (15), one arrives at

$$\rho \frac{\partial^2 u}{\partial \rho^2} = 2\frac{a}{(2\pi)^2}\left(\sum_\nu \frac{\partial a}{\partial G_\nu}\frac{\partial G_\nu}{\partial u}\right)\frac{\partial u}{\partial \beta} = B(\rho, u)\frac{\partial u}{\partial \beta} \tag{16}$$

once a, $\partial a/\partial G_\nu$, and $\partial G_\nu/\partial u$ have been expressed as functions of ρ and u. The required expressions are obtained by implicit differentiation of a set of non-linear equations in the G_ν and u that are summarized in [30]. Equation (16) is now a quasilinear PDE of diffusion type which has to be solved numerically (as described in detail in [9]) on a (β, ρ) grid, $[0, \beta_f] \times [0, \rho_0]$, with a suitable initial condition (for $\beta = 0$) and suitable boundary conditions (here, the high-temperature approximation for the upper density limit $\rho_0\sigma^3 = 1$). In contrast to conventional liquid-state theories, the SCOZA can be solved up to the critical point; special care has to be taken in the region of instability (characterized by a negative compressibility) which has to be excluded from the region of integration.

From the solution of the PDE (16) we obtain the full information about the structure and the thermodynamic properties of the system. For instance, the pressure P and the chemical potential μ (i.e. two quantities required to determine the phase behaviour) are calculated from

$$\frac{\partial}{\partial \beta}(\beta P) = -u + \rho\frac{\partial u}{\partial \rho} \tag{17}$$

$$\frac{\partial}{\partial \beta}(\beta \mu) = \frac{\partial u}{\partial \rho} \tag{18}$$

via thermodynamic integration.

2.2. SCOZA—the binary symmetric mixture

In the case of a binary mixture, the OZ relation (3) and the core condition (4) for the partial PDFs $g_{ij}(r)$ are generalized in an obvious way. The closure relations for the direct correlation functions (5), generalized to the binary case and restricting ourselves to one single Yukawa tail, now read

$$c_{ij}(r) = c_{\mathrm{HC};ij}(r) + K_{ij}(\rho, T, x)w_{ij}(r) \qquad \text{for } r > \sigma_{ij}. \tag{19}$$

In the *general* binary case the three as yet unknown functions $K_{ij}(\rho, T, x)$ are determined via the following three (partial) consistency relations:

$$\frac{\partial^2 u}{\partial\rho_i\,\partial\rho_j} = \frac{\partial}{\partial\beta}[-\tilde{c}_{ij}(q=0)] \qquad i, j = 1, 2. \tag{20}$$

Again, u is calculated via the energy route (generalized expression (7)). So one arrives at a coupled set of three PDEs for the three unknown functions K_{ij}. Due to the complexity of the *general* binary case, we restrict ourselves here to the binary *symmetric* case, i.e. we assume that

$$\Phi_{11}(r) = \Phi_{22}(r) = \frac{1}{\alpha}\Phi_{12}(r). \tag{21}$$

This leads to considerable simplifications: first, $\sigma_{ij} = \sigma$ and hence we can use $c_{\mathrm{HC};ij}(r) = c_{\mathrm{HC}}(r)$, i.e. the Waisman parametrization for the direct correlation function of the HC reference system mentioned above; second, the as yet undetermined functions $K_{ij}(\rho, T, x)$ satisfy the following symmetry relations:

$$K_{11}(\rho, T, x) = K_{22}(\rho, T, 1-x) \tag{22}$$
$$K_{12}(\rho, T, x) = K_{12}(\rho, T, 1-x). \tag{23}$$

Under the additional, simplifying assumption $K_{11}(\rho, T, x) = K_{12}(\rho, T, x)$ we end up with one function $K(\rho, T, x)$, that is symmetric and that is related to the K_{ij} via

$$K(\rho, T, x) = K_{ij}(\rho, T, x). \tag{24}$$

We now require only one consistency relation, obtained from a suitable linear combination of the partial consistency relations (20), e.g.,

$$\rho\frac{\partial^2 u}{\partial\rho^2} = \frac{\partial}{\partial\beta}\left(1 - \frac{1}{\rho}\sum_{ij}\rho_i\rho_j\tilde{c}_{ij}(q=0)\right) = \frac{\partial}{\partial\beta}\left(\frac{1}{\chi_{\mathrm{red}}}\right). \tag{25}$$

By using the assumption $K_{11} = K_{22}$, we have added an additional approximation that goes beyond the definition of the SCOZA, and we must expect the resulting numerical results to be less highly accurate than those obtained in applications that use nothing but the ansatz that defines the SCOZA. To check the accuracy of this additional approximation, a detailed comparison with Monte Carlo simulations is planned [32]. Nevertheless, our binary mixture results capture the full range of critical and tricritical behaviour that one would expect in an exact analysis.

The derivation of the SCOZA PDE follows, from here on, similar lines to in the one-component case, but is considerably more complex; in addition, actual calculations require a substantial amount of computing time. Again, the compressibility can be expressed by the coefficients a_i of the factor functions $Q_{ij}(r)$, so (16) now reads

$$\rho\frac{\partial^2 u}{\partial\rho^2} = 2\sum_j x_j\frac{a_j}{(2\pi)^2}\left(\sum_{v;rs}\frac{\partial a_j}{\partial G_{v;rs}}\frac{\partial G_{v;rs}}{\partial u}\right)\frac{\partial u}{\partial\beta} = B(\rho, u)\frac{\partial u}{\partial\beta}. \tag{26}$$

The a_j, $\partial a_j/\partial G_{\nu;rs}$, and $\partial G_{\nu;rs}/\partial u$ have to expressed as functions of ρ and u. The PDE (26) is a quasilinear PDE of diffusion type which has to be solved numerically for different x-values on a (β, ρ) grid, $[0, \beta_f] \times [0, \rho_0]$: the initial condition ($\beta = 0$) is obtained by making use of the fact that the direct correlation functions $c_{ij}(r)$ coincide with those of a one-component HC system; for the boundary condition on the high-density side we take again the HTA. As in the one-component case, we have to exclude the region where thermodynamic stability requirements are not satisfied. However, we now have to distinguish between two types of instability, i.e. material and mechanical instability (for details cf [30]).

Thermodynamic properties are calculated—similarly to in the one-component case—via thermodynamic integration:

$$\frac{\partial}{\partial\beta}(\beta P) = -u + \rho\frac{\partial u}{\partial\rho} \tag{27}$$

$$\frac{\partial}{\partial\beta}(\beta\mu_1) = \frac{\partial u}{\partial\rho} + \frac{(1-x)}{\rho}\frac{\partial u}{\partial x} \tag{28}$$

$$\frac{\partial}{\partial\beta}(\beta\mu_1) = \frac{\partial u}{\partial\rho} - \frac{x}{\rho}\frac{\partial u}{\partial x}. \tag{29}$$

The symmetry of the system induces symmetry relations in the correlation functions and hence in the thermodynamic properties. For instance, for the chemical potentials and for the pressure we find

$$\mu_1(\rho, T, x) = \mu_2(\rho, T, 1-x) \tag{30}$$

$$P(\rho, T, x) = P(\rho, T, 1-x). \tag{31}$$

3. Results

3.1. One-component case

3.1.1. Phase behaviour of fullerenes. The standard test system of liquid-state theories is the LJ system. In [6] the LJ interaction was approximated by a suitable HC–two-Yukawa-tail interaction; on the basis of this model it was shown that the SCOZA is indeed able to reproduce the computer simulation data for the critical point and the liquid–gas coexistence curve very accurately.

In this contribution we focus on the Girifalco potential, a sphericalized interaction between the C_{60} molecules derived in [20]: this was done under the assumption of a uniform distribution of the carbon atoms on the surface of a rigid sphere (of diameter R) and a LJ interaction between the carbon atoms of different molecules. The potential is given by

$$\Phi(r) = -\alpha\left[\frac{1}{s(s-1)^3} + \frac{1}{s(s+1)^3} - \frac{2}{s^4}\right] + \beta\left[\frac{1}{s(s-1)^9} + \frac{1}{s(s+1)^9} - \frac{2}{s^{10}}\right] \tag{32}$$

with $s = \frac{r}{R}$, $\alpha = \frac{N^2A}{12R^6}$, $\beta = \frac{N^2B}{90R^{12}}$, where N is the number of carbon atoms of the fullerene molecule; $A = 32 \times 10^{-60}$ erg cm^6 and $B = 55.77 \times 10^{-105}$ erg cm^{12} are the parameters of the LJ potential between the carbon atoms. We have summarized the parameters R, α, and β, along with R_0 and ϵ (i.e., the zero and the depth of the potential) in table 1. In figure 1 we show a LJ and a Girifalco potential (C_{60}) in reduced units: potential energies are expressed in units of the well depth, the range in units of the zero of the potential. Three facts become obvious: the repulsive part of the Girifalco potential is much stiffer, and its attractive part is much shorter ranged and—when comparing the depth in 'real' units—much deeper than the LJ interaction.

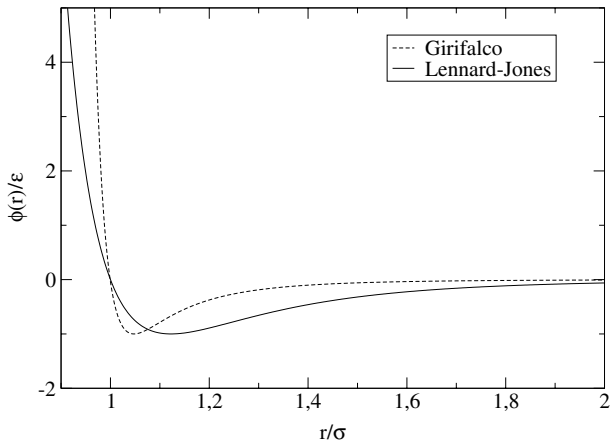

Figure 1. The LJ potential and Girifalco potential (C_{60}), as labelled, in reduced units: potential energies are expressed in units of the well depth (ϵ), the range in units of the zero of the potentials (σ).

Table 1. Parameters of the Girifalco potential (32) for model C_{60} and C_{70} studied in this contribution (see the text). Distances are given in nm, ϵ/k_B in K, and α and β are in units of 10^{-15} and 10^{-18} erg, respectively [34].

	R	R_0	ϵ/k_B	α	β
C_{60}	0.71	0.9599	3218	74.94	135.95
C_{70}	0.762	1.011	3653	66.7	79.23

In order to make $\Phi(r)$ ready for use in the extended SCOZA framework, we proceed in the following way: we replace the harsh repulsion of $\Phi(r)$ for $r < R_0$ by a HC potential of diameter σ and approximate for $r > R_0$ the purely attractive part of $\Phi(r)$ by a linear combination of three or four Yukawa tails, leading thus to $w(r)$ of the form (2). Solution of the SCOZA gives the critical point and the coexistence curve; the triple point is estimated from the intersection of the liquid–gas coexistence curve with the freezing line; the latter is obtained from an entropic criterion [33] which is known to give accurate results. The thermodynamic and structural data required in this criterion are readily provided by the SCOZA.

The SCOZA results for the critical and the triple-point parameters are summarized, along with data from Gibbs ensemble Monte Carlo (GEMC) simulations [34, 35], in table 2. We find excellent agreement for the location of the critical point. Also the results for ρ_t agree very well; however, discrepancies are observed for T_t: this might be due to the fact that the GEMC results are based on an *extrapolation* of the gas–liquid coexistence curve, while our coexistence curve is *determined* down to and even below T_t. Two remarks are in order:

(i) The particular features of the Girifalco potential mentioned above can lead to numerical complications in other liquid-state theories, such as the HRT [21]. Therefore the fact that the SCOZA is able to reproduce simulation results very accurately can be considered as a further indication of the wide applicability of this advanced liquid-state theory.

(ii) The specific features of the Girifalco potential have led to a still ongoing discussion on the existence of the liquid phase in fullerenes; for details we refer the reader to [34], one of the most recent publications on this subject.

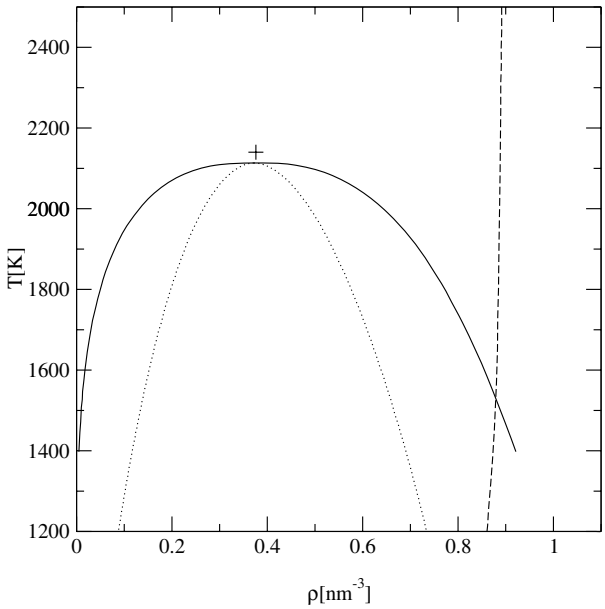

Figure 2. The phase diagram of model C_{60} calculated via the SCOZA. Full curve—liquid–vapour binodal; dotted curve—spinodal; broken line—freezing line as estimated from an entropic criterion (see the text); symbol—critical point from GEMC simulations [35].

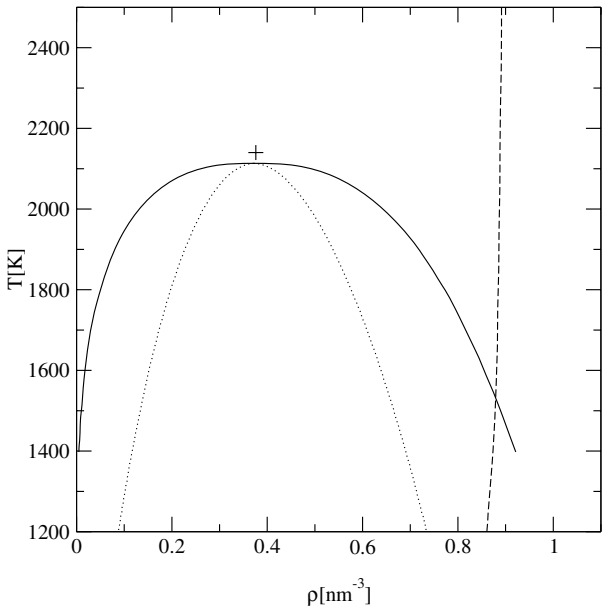

Figure 3. The phase diagram of model C_{70} as calculated via the SCOZA. Full curve—liquid–vapour binodal; dotted curve—spinodal; broken curve—freezing line as estimated from an entropic criterion (see the text); symbol—critical point from GEMC simulations [34].

3.1.2. Phase behaviour of systems with density-dependent potentials. Having found further evidence that the SCOZA is able to localize the critical point of a simple fluid very accurately,

Table 2. Results for the triple point and the critical point of model C_{60} and C_{70} described via the Girifalco potential (see the text): SCOZA versus Gibbs ensemble Monte Carlo (GEMC) simulations (for different particle numbers N).

		GEMC [35]		
C_{60}	SCOZA	$N = 300$	$N = 600$	$N = 1500$
T_t (K)	1388	—	1500–1700	—
ρ_t (nm^{-3})	1.03	—	0.91–1.0	—
T_c (K)	1957	1924	1927	1941
ρ_c (nm^{-3})	0.432	0.39	0.40	0.42
C_{70}	SCOZA		GEMC [34]	
T_t (K)	1531		1650	
ρ_t (nm^{-3})	0.879		0.88	
T_c (K)	2113		2140	
ρ_c (nm^{-3})	0.372		0.376	

we are now able to study the following problem on a *quantitative* level: we consider an explicitly density-dependent pair potential, $\Phi(r) = \Phi_{\rm HC}(r) + w(r;\rho)$, using for $w(r;\rho)$ a Yukawa potential, i.e.

$$w(r;\rho) = -\frac{\epsilon}{r}\exp[-z(\rho)(r-\sigma)] \qquad r > \sigma. \tag{33}$$

The density dependence is introduced via the inverse screening length $z(\rho)$, using the same functional form as the one proposed for the exponent of the inverse power potential of a recent van der Waals study by Tejero and Baus [36]:

$$z(\rho)\sigma = 1.6 + \frac{z_0\sigma - 1.6}{1 - \frac{2}{3}\alpha\rho + \frac{1}{6}\alpha^2\rho^2}. \tag{34}$$

Two parameters enter this expression, $z_0\sigma$ and α; in figure 4 we show $z(\rho)$ for the two different values of $z_0\sigma$ considered in this study and for one selected α-value. We observe a non-monotonic behaviour for $z(\rho)$ as a function of ρ, where, depending on the value of $z_0\sigma$, the maximum is more or less pronounced.

It should be pointed out that for the particular case of an explicitly density-dependent potential the standard relations for the thermodynamic routes have to be reconsidered. In fact, the usual expression for the virial has to be reformulated, while the energy and the compressibility routes are still valid. Since the SCOZA is based on the latter two routes, we can leave the virial route aside; if the pressure is required it can be obtained via thermodynamic integration of the energy (cf (18)).

In the mean-field study mentioned above, the authors observed for selected sets of parameters a gas–liquid and a liquid–liquid phase transition, each with its own critical points; in some cases these transitions were metastable, covered (partially) by a stable vapour/liquid–solid transition. In a subsequent study [37] based on computer simulations and conventional liquid-state theories, similar results were observed; agreement between the different methods was rather on a qualitative level.

The SCOZA offers us the possibility to study these phenomena on a *quantitative* level. We have solved the SCOZA for the above interaction (33), (34) and have determined the phase behaviour. Indeed, for suitable parameters $z_0\sigma$ and α we could observe a gas–liquid and a liquid–liquid transition, each with its own critical point. The parameter range where this double criticality can be observed is, with respect to both $z_0\sigma$ and α, rather narrow. In figure 5

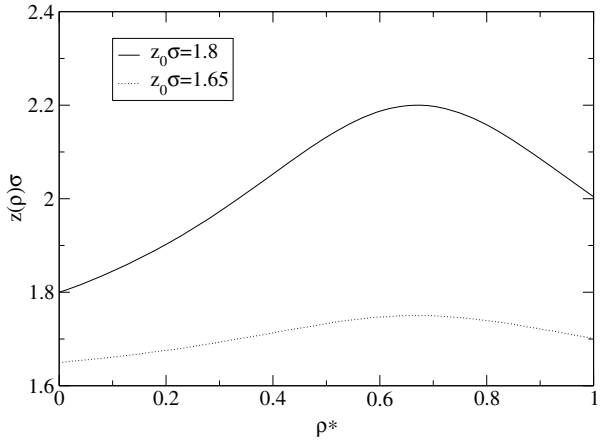

Figure 4. The density dependence of the inverse screening length $z(\rho)$ of the HCY potential of equation (33), given by equation (34) for two selected values of $z_0\sigma$ (as labelled); $\alpha = 5.7v_0$ with v_0 being the hard-sphere volume.

we show a series of phase diagrams, fixing $z_0\sigma = 1.8$ and varying α from 0 (corresponding roughly to a density-*in*dependent $z\sigma \equiv 1.8$) to large α (corresponding to a density-*in*dependent $z\sigma \equiv 1.6$). Around $\alpha \sim 5.5v_0$ (v_0 being the volume of the sphere), we observe two clearly separated phase transitions, the related two critical points, and the triple point (marked by a kink in the coexistence curve). A closer analysis shows that the α-range where this phenomenon is observed is only $5.34 \leqslant \alpha/v_0 \leqslant 5.75$. Note that as we vary α from zero to infinity (approximated by $\alpha = 100v_0$), the critical parameters, $T_{\rm cr}$ and $\rho_{\rm cr}$, vary strongly with α. In addition we have found that the position of the two critical points can be shifted via z_0. To be more specific, we succeeded in merging the two critical points into a confluent critical point. This situation is shown in figure 6 where we depict three phase diagrams for $z_0\sigma = 1.65$. For the intermediate value of α, we observe a confluent critical point. In figure 7 we have shown the coexistence densities ρ_l and ρ_v as functions of $(-t)^{1/4}$: the two curves are nearly straight lines. This is a clear indication that the critical exponent $\beta \sim 1/4$, which is the expected exact value for a three-dimensional system.

3.2. Binary symmetric case

We present results for the phase diagram of a binary symmetric mixture. As a consequence of the restricted number of parameters, the phase behaviour of such a system can be studied very easily in a systematic way; the parameter that triggers the phase behaviour is α, the ratio between the unlike and the like interaction, introduced in (21). Despite its simplicity, we encounter a surprisingly rich phase behaviour for this system, including phenomena such as critical lines, critical end-points (CEP), and tricritical points. A qualitative study of these phenomena based on a mean-field model has been presented by Wilding *et al* [38]. We expect four phases, the vapour (G), the mixed fluid (MF), and two phases of a demixed fluid (DF)—a 1-rich and a 2-rich fluid; the latter ones are often counted—as a consequence of the symmetry with respect to x—as one single phase.

To calculate the phase diagram, the equations that determine coexistence, i.e. equal chemical potentials and equal pressure of the coexisting phases at a given temperature, have to be solved. Characterizing coexisting phases by (ρ, x) and (ρ', x') we proceed as follows:

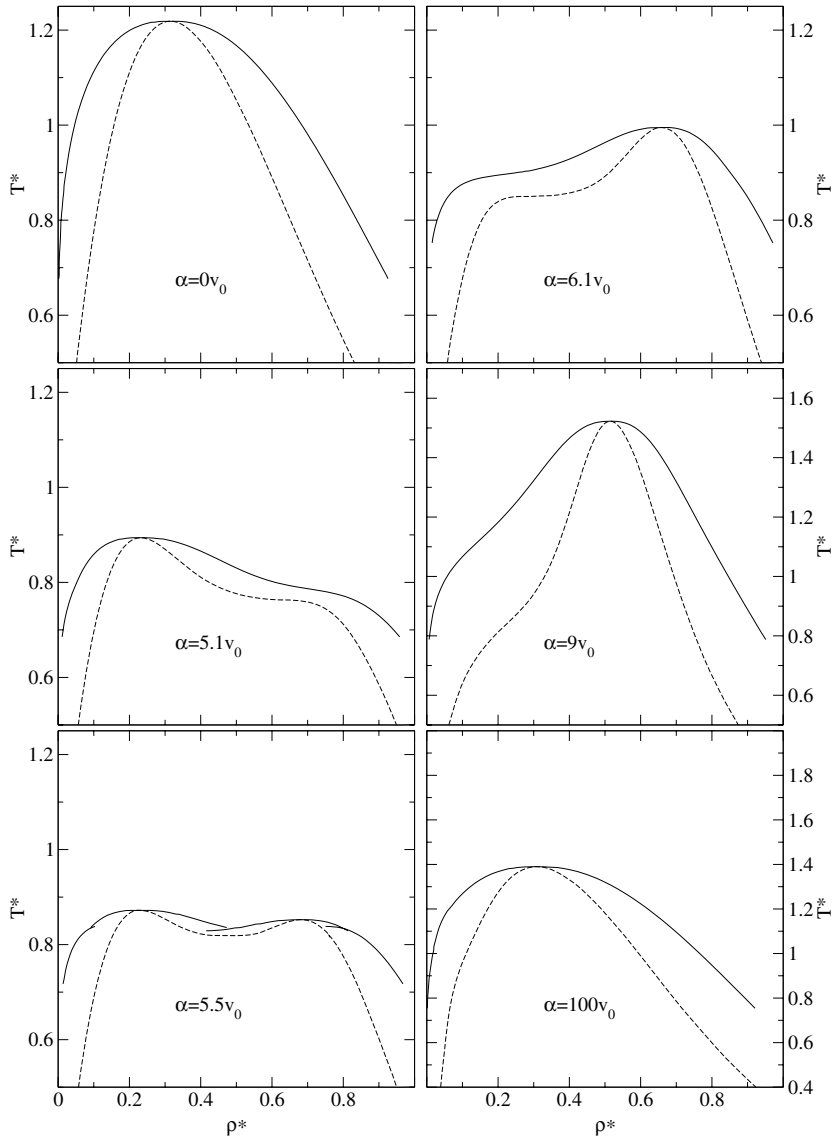

Figure 5. Phase diagrams of a HCY potential with an explicitly density-dependent screening length (see the text) for $z_0\sigma = 1.8$ and α-values as indicated (see equation (34)). $\alpha = 0$ corresponds to a density-independent screening length $z\sigma \equiv 1.8$, while $\alpha = 100v_0$ (approximating the case $\alpha = \infty$) corresponds to a density-independent screening length $z\sigma \equiv 1.6$. Full curves—binodals; broken curves—spinodals; $T^\star = k_B T\sigma/\epsilon$, $\rho^\star = \rho\sigma^3$.

the G–MF coexistence curve is obtained by solving the set of equations

$$\mu_i(\rho, T, x = 1/2) \equiv \mu(\rho, T, x = 1/2) = \mu(\rho', T, x = 1/2) \tag{35}$$
$$P(\rho, T, x = 1/2) = P(\rho', T, x = 1/2). \tag{36}$$

For the G–MF and the MF–DF transitions we proceed in two steps: first we determine the phase diagram of the demixing transition, i.e. at a given temperature T we search for two coexisting states with the same fluid density but different composition by fixing $\rho = \rho'$ and by

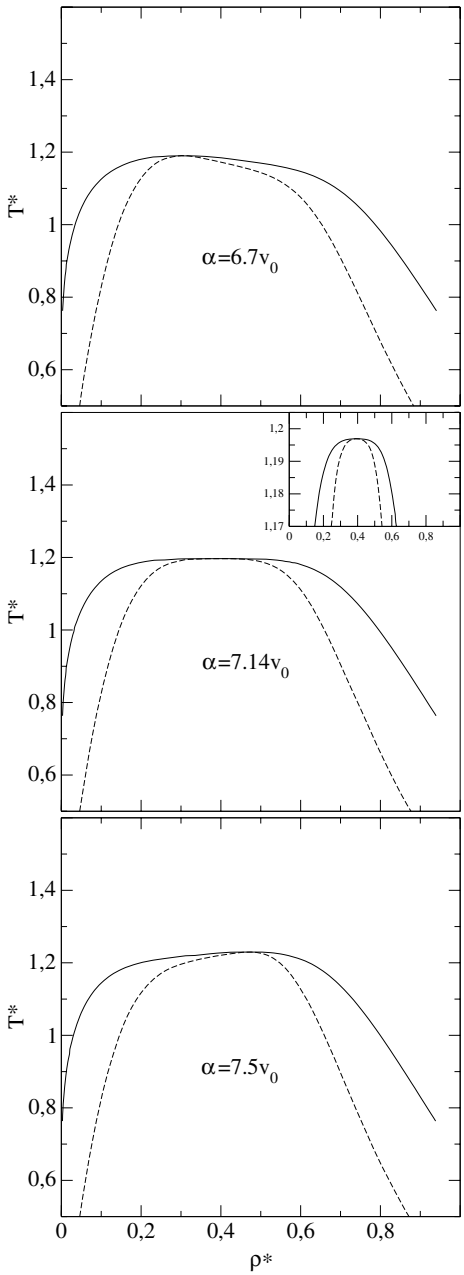

Figure 6. Phase diagrams of a HCY potential with an explicitly density-dependent screening length (see the text) for $z_0\sigma = 1.65$ and α-values as indicated. Full curves—binodals; broken curves—spinodals; $T^\star = k_B T\sigma/\epsilon$, $\rho^\star = \rho\sigma^3$. The inset ($\alpha = 7.14v_0$) shows an enlargement of the 'near-tricritical' region.

determining concentrations x and $x' = 1 - x$ of the coexisting phases. Then the equilibrium condition for the pressure is automatically fulfilled, while the equilibrium conditions for the

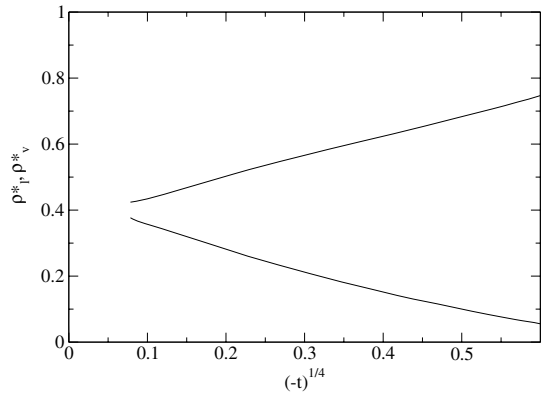

Figure 7. Coexistence densities $\rho_l^\star = \rho_l \sigma^3$ and $\rho_v^\star = \rho_v \sigma^3$ as functions of $(-t)^{1/4}$ for the phase diagram shown in figure 6 ($\alpha = 7.14 v_0$).

chemical potentials become, at given T and ρ,

$$\mu_1(\rho, T, x) = \mu_2(\rho, T, x) \tag{37}$$

which defines the line $x(\rho)$ of the second-order demixing transition, if it exists. Along this line the chemical potentials of the two species are equal by construction and are denoted by $\mu[T, \rho, x(\rho)]$. In a second step the solution of the two equations

$$\mu[\rho, T, x = 1/2] = \mu[\rho', T, x(\rho')] \tag{38}$$
$$P[\rho, T, x = 1/2] = P[\rho', T, x(\rho')] \tag{39}$$

gives the density ρ of the G or MF and the density ρ' of the DF with concentrations $x(\rho')$ and $1 - x(\rho')$, in equilibrium. In figure 8 we present the projection of the phase diagram of the binary symmetric mixtures onto the (T, ρ) plane for three different values of α (as indicated).

The parameter α entirely triggers the phase behaviour of the system. If $\alpha \geqslant 1$, we observe only a G–MF transition, the critical line is absent. The situation is more interesting and more complex for $\alpha < 1$: here we have a competition between the G–MF transition and the demixing transition; the latter is characterized by the λ-line, i.e. the critical line of the demixing transitions. Depending on the interplay of these two types of phase transition, one can distinguish three types of phase diagram (see figure 8).

(i) For type I, the λ-line approaches the G–MF coexistence curve well below the critical point and intersects the first order G–MF curve at a CEP: here, a critical liquid coexists with a non-critical gas. Above T_{CEP} a gas and a homogeneous liquid of intermediate density coexist, becoming identical at the G–MF critical point. Upon increasing the densities, the liquid demixes as one crosses the λ-line. The (full) curve below the CEP temperature (cf bottom panel in figure 8) is a triple line where a gas, a 1-rich liquid, and a 2-rich liquid coexist.

(ii) For type III the λ-line meets the G–MF line at the G–MF critical point. In that case the first-order transition between the gas and the mixed liquid is absent and the λ-line ends at a tricritical point where three phases become critical at the same time: a gas, a 1-rich liquid, and a 2-rich liquid. Here, two order parameters—the difference between the coexisting liquid and vapour densities and the concentration difference—vanish at the same time. Tricriticality is, by the way, a specific feature of the symmetric model, which is not encountered in a general binary fluid [39].

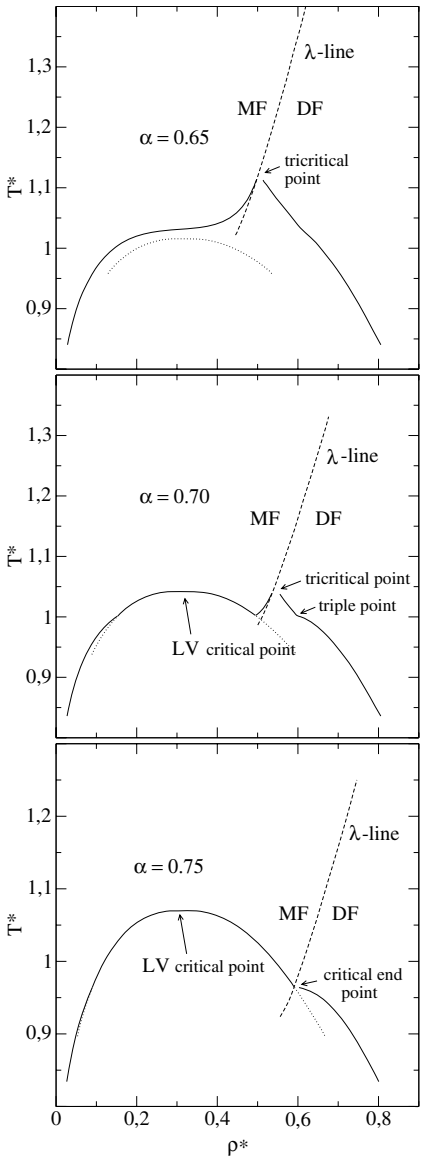

Figure 8. The phase diagram of a binary symmetric mixture (as defined in the text), projected onto the ($T^\star$, $\rho^\star$) plane for three different α-values as indicated; $T^\star = k_B T\sigma/K_{11}$, $\rho^\star = \rho\sigma^3$. Regions where the different phases exist are labelled by acronyms (MF—mixed fluid; DF—demixed fluid). Full curves—binodals; dotted curves—metastable G–MF coexistence curves.

(iii) Finally, type II represents the intermediate case, where the λ-line approaches the G–MF coexistence curve slightly below the critical point. As in type I, one finds a critical point of the G–MF transition and, like for type III, a tricritical point. In addition, this type is characterized by a triple point where—to be correct—four phases coexist: a gas, a mixed liquid at intermediate density, and a 1-rich and a 2-rich liquid at high density. In figure 8 the α-values are chosen such that each of the above-defined phase diagram types is represented. Note that in contrast to conventional liquid-state methods (cf [40]), the SCOZA can be solved also in regions very close to the critical points.

Concluding, it should be pointed out that similar archetypes of phase diagrams are also encountered in other liquid systems with completely different interatomic interactions, such as the Heisenberg fluid [41] and the Stockmayer fluid [42].

4. Conclusions

We have presented a generalization of the formalism of the SCOZA, a liquid-state theory that is able to predict the location of the critical point and of the liquid–vapour coexistence curves of a simple fluid with high accuracy. By including formally an arbitrary number of Yukawa tails in the attractive part of the HC interaction of the system we are now able to treat systems with potentials that can be approximated by a suitable linear combination of Yukawa tails. This generalization is realized by fully maintaining the attractive advantages of the availability of the (semi-)analytic solution of the MSA for a HC–multi-Yukawa-tail fluid. We first tested the accuracy of our SCOZA version in a direct comparison with accurate GEMC results for model fullerenes and found excellent agreement for the critical point. In view of this, we then determined the phase behaviour of a HC–one-Yukawa-tail system where the inverse screening length $z(\rho)$ is explicitly density dependent; to be more specific, $z(\rho)$ shows a non-monotonic behaviour as a function of the density ρ. Depending on the parameters that define the functional dependence of $z(\rho)$ on ρ, we observe up to two critical points that can even be merged into a tricritical point; evidence for this is found from an analysis of the critical exponent β. We observe a value for β that is consistent with $1/4$, i.e. the mean-field value for a tricritical point, which is also the expected exact value in a three-dimensional system. Finally, we apply the SCOZA to the case of a binary symmetric mixture, for which an additional approximated relation was used to close our equations. We are able to identify three archetypes of phase diagrams that are characterized by the loci where the critical line of the demixing transitions intersects the first-order liquid–vapour coexistence line. In contrast to conventional microscopic liquid-state theories, such as the optimized random-phase approximation and integral equation theories, the SCOZA can be solved in regions very close to the critical points.

Acknowledgments

This work was supported by the FWF (Österreichische Forschungsfonds) under Project Nos P13062-TPH, P14371-TPH, P15758-TPH, and W0004. ESP acknowledges gratefully the hospitality of the Department of Chemistry at Stony Brook where part of this work was performed. GS gratefully acknowledges the support of the Division of Chemical Sciences, Office of Basis Energy Sciences, Office of Energy Research, US Department of Energy. Stimulating discussions with Dr A A Louis (Cambridge) and Prof H Löwen (Düsseldorf) are gratefully acknowledged.

References

[1] Hansen J-P and McDonald I R 1986 *Theory of Simple Liquids* 2nd edn (New York: Academic)
[2] Caccamo C 1996 *Phys. Rep.* **274** 1
[3] Høye J S and Stell G 1977 *J. Chem. Phys.* **67** 439
[4] Høye J S and Stell G 1984 *Mol. Phys.* **52** 1071
[5] Pini D, Stell G and Wilding N B 1998 *Mol. Phys.* **95** 483
[6] Pini D, Stell G and Wilding N B 2001 *J. Chem. Phys.* **115** 2702
[7] Parola A and Reatto L 1995 *Adv. Phys.* **44** 211
[8] Dickman R and Stell G 1996 *Phys. Rev. Lett.* **77** 996

[9] Pini D, Stell G and Dickman R 1998 *Phys. Rev.* E **57** 2862
[10] Borge A and Høye J S 1998 *J. Chem. Phys.* **108** 4516
Høye J S and Borge A 1998 *J. Chem. Phys.* **108** 8830
[11] Grollau S 2001 *PhD Thesis* Université Pierre et Marie Curie
Grollau S, Kierlik E, Rosinberg M-L and Tarjus G 2001 *Phys. Rev.* E **63** 411111
Grollau S, Rosinberg M-L and Tarjus G 2001 *Physica* A **296** 460
[12] Høye J S and Stell G 1997 *Physica* A **244** 176
[13] Høye J S and Stell G 1997 *Physica* A **247** 497
[14] Pini D, Høye J S and Stell G 2002 *Physica* A **307** 469
[15] Dickman A G and Stell G 2002 *Mol. Phys.* at press
[16] Pini D, Stell G and Høye J S 1998 *Int. J. Thermophys.* **19** 561
[17] Høye J S, Pini D and Stell G 2000 *Physica* A **279** 213
[18] Waisman E, Høye J S and Stell G 1976 *Chem. Phys. Lett.* **40** 514
Høye J S, Stell G and Waisman E 1976 *Mol. Phys.* **32** 209
Høye J S and Stell G 1984 *Mol. Phys.* **52** 1057
[19] Arrieta E, Jedrzejek C and Marsh K N 1991 *J. Chem. Phys.* **95** 6806
[20] Girifalco L A 1992 *J. Chem. Phys.* **95** 5370
Girifalco L A 1992 *J. Chem. Phys.* **96** 858
[21] Reiner A 2002 private communication
[22] Ornstein L S and Zernike F 1914 *Proc. Acad. Sci. (Amsterdam)* **17** 1452
[23] Waisman E 1973 *Mol. Phys.* **25** 45
[24] Wertheim M 1964 *The Equilibrium Theory of Classical Fluids* ed H Frisch and J Lebowitz (New York: Benjamin) p II-268
[25] Baxter R J 1968 *Aust. J. Phys.* **21** 563
[26] Blum L and Høye J S 1978 *J. Stat. Phys.* **19** 317
[27] Blum L 1980 *J. Stat. Phys.* **22** 661
[28] Blum L, Vericat F and Herrera-Pacheco J N 1992 *J. Stat. Phys.* **66** 249
[29] Blum L and Herrera J N 1998 *Mol. Phys.* **95** 425
[30] Schöll-Paschinger E 2002 *PhD Thesis* Technische Universität Wien (unpublished thesis, available from the homepage: http://tph.tuwien.ac.at/∼paschinger/ and download 'PhD')
[31] Pastore G 1988 *Mol. Phys.* **55** 187
[32] Schöll-Paschinger E, Levesque D, Weis J-J and Kahl G, at press
[33] Giaquinta P V and Giunta G 1992 *Physica* A **187** 145
Giaquinta P V, Giunta G and Giarritta S O 1992 *Phys. Rev.* A **45** 6966
[34] Abramo M C, Caccamo C, Costa D and Pellicane G 2001 *Europhys. Lett.* **54** 468
[35] Caccamo C, Costa D and Fucile A 1997 *J. Chem. Phys.* **106** 255
[36] Tejero C F and Baus M 1998 *Phys. Rev.* **57** 4821
[37] Almarza N, Lomba E, Ruiz G and Tejero C F 2001 *Phys. Rev. Lett.* **86** 2038
[38] Wilding N B, Schmid F and Nielaba P 1998 *Phys. Rev.* E **58** 2201
[39] van Konynenburg P H and Scott R L 1980 *Phil. Trans. R. Soc.* A **51** 495
[40] Schöll-Paschinger E, Levesque D, Weis J-J and Kahl G 2001 *Phys. Rev.* E **64** 011502
Schöll-Paschinger E, Levesque D, Kahl G and Weis J-J 2001 *Europhys. Lett.* **55** 178
[41] Weis J-J, Nijmeijer M J P, Tavares J M and Telo da Gama M M 1997 *Phys. Rev.* E **55** 436
Tavares J M, Telo da Gama M M, Teixeira P I C, Weis J-J and Nijmeijer M J P 1995 *Phys. Rev.* E **52** 1915
[42] Groh B and Dietrich S 1994 *Phys. Rev. Lett.* **72** 2422
Groh B and Dietrich S 1999 *New Approaches to Problems in Liquid State Theory (NATO Science Series)* ed C Caccamo, J-P Hansen and G Stell (Dordrecht: Kluwer)